

Criticality-Guided Efficient Pruning in Spiking Neural Networks Inspired by Critical Brain Hypothesis

Author Name

Affiliation

email@example.com

Abstract

Spiking Neural Networks (SNNs) have gained considerable attention due to the energy-efficient and multiplication-free characteristics. The continuous growth in scale of deep SNNs poses challenges for model deployment. Network pruning reduces hardware resource requirements of model deployment by compressing the network scale. However, existing SNN pruning methods cause high pruning costs and performance loss because the pruning iterations amplify the training difficulty of SNNs. In this paper, inspired by the critical brain hypothesis in neuroscience, we propose a regeneration mechanism based on the neuron criticality for SNN pruning to enhance feature extraction and accelerate the pruning process. Firstly, we propose a low-cost metric for the criticality in SNNs. Then, we re-rank the pruned structures after pruning and regenerate those with higher criticality to obtain the critical network. Our method achieves higher performance than the current state-of-the-art (SOTA) method with up to 95.26% reduction of pruning cost. Moreover, we investigate the underlying mechanism of our method and find that it efficiently selects potential structures and learns the consistent feature representation.

1 Introduction

Spiking Neural Networks (SNNs) have received considerable attention in recent years [Wu *et al.*, 2019; Zheng *et al.*, 2021] as the third generation of neural networks [Maass, 1997]. SNNs are widely employed in resource-constrained hardware [Akopyan *et al.*, 2015; Davies *et al.*, 2018; Pei *et al.*, 2019], relying on energy-efficient and multiplication-free advantages from sparse spike signals.

The limited computational and storage resources of hardware pose challenges to implementing deep SNNs with large-scale parameters. Network pruning provides a potential solution to address resource issues. There have been a lot of efforts to unstructured pruning for SNNs. Methods inspired by the human brain include modeling synaptic regeneration processes [Kundu *et al.*, 2021] and dendritic motion [Kappel

| Method | #Epoch | Acc. (%) |
|--------------------------------------|--------|----------|
| Grad R [Chen <i>et al.</i> , 2021] | 2048 | 67.47 |
| IMP [Kim <i>et al.</i> , 2022] | 3380 | 70.54 |
| RCMO-SNN [Chen <i>et al.</i> , 2023] | 3100 | 72.67 |
| NDSNN [Huang <i>et al.</i> , 2023] | 300 | 68.95 |
| This work | 200 | 73.01 |

Table 1: Test accuracy and required pruning epochs on ResNet19 with about 95% sparsity for CIFAR100 using different pruning methods.

et al., 2015]. Qi *et al.* [2018] designed connection gates during the training process for synaptic pruning. Recent efforts reference techniques from Artificial Neural Network (ANN) pruning. Kim *et al.* [2022] explored the "lottery ticket" hypothesis in SNN pruning with Iterative Magnitude Pruning (IMP). Deng *et al.* [2021] combined Spatio-Temporal Back-propagation (STBP) and Alternating Direction Method of Multipliers (ADMM) and proposed an activity-based regularization method. Grad R [Chen *et al.*, 2021] improved the Deep R method by introducing a weight regeneration mechanism. RCMO-SNN [Chen *et al.*, 2023] proposed an end-to-end Minimax optimization method for sparse learning.

However, current state-of-the-art (SOTA) pruning methods for SNNs cause high pruning costs and performance loss. Table 1 summarizes the required epochs and pruned accuracy on ResNet19 with about 95% sparsity for CIFAR100 using different pruning methods. Existing SOTA methods require over 2000 epochs [Chen *et al.*, 2021; Kim *et al.*, 2022; Chen *et al.*, 2023]. Huang *et al.* [2023] develop NDSNN based on sparse training, reducing pruning cost to 300 epochs but with a significant loss of accuracy. Other efforts to reduce pruning costs include compressing timesteps during the pruning process [Kim *et al.*, 2022, 2023]. However, these efforts only achieve acceleration ratios of 1.12 to 1.59 and lead to significant accuracy losses.

The high cost of pruning comes from the expensive pruning iterations [Chen *et al.*, 2021; Kim *et al.*, 2022; Chen *et al.*, 2023]. Multiple rounds of pruning and fine-tuning are employed in SOTA SNN pruning methods to achieve high-performance pruned models. However, the utilization of sparse spike signals in SNNs introduces problems like

spike and gradient vanishing, which hinder both forward and backward propagation during SNN training, consequently leading to inefficient information passing and feature extraction [Zheng *et al.*, 2021; Wu *et al.*, 2019; Shrestha *et al.*, 2021]. The iterative pruning exacerbates this problem, requiring the long recovery time after each pruning round [Kim *et al.*, 2022; Chen *et al.*, 2023], or forcing magnitude reduction of single pruning step for rapid recovery [Chen *et al.*, 2021]. Both lead to a multiplication of pruning costs, still accompanying a loss in accuracy.

In this paper, we are the first to leverage criticality to improve feature extraction and achieve high-efficiency pruning for SNNs. The critical brain hypothesis [Turing, 2009] reveals that brain neurons with the critical state are highly sensitive to inputs and exhibit enhanced information transmission, associated with the complex feature extraction and learning process of the brain [Kinouchi and Copelli, 2006; Beggs, 2008; Shew *et al.*, 2009; Beggs and Timme, 2012]. Inspired by this, our goal is to leverage the advantages of criticality to enhance feature extraction and speed up the pruning process in SNN pruning. Based on the association between criticality and the barely-excitable state of a single neuron [Gal and Marom, 2013], we propose a metric for neuron criticality and further relate it to the surrogate function derivative to avoid additional computational costs. We then design a regeneration mechanism based on neuron criticality to introduce criticality into the pruning and fine-tuning iterations and preserve critical neurons. The proposed method is evaluated on unstructured and structured pruning and achieves SOTA performances. Moreover, we explore the underlying impact of our method and find that it efficiently selects potential structures and improves the uniformity of features.

In summary, our key contributions are as follows:

- Inspired by the critical brain hypothesis in neuroscience, we propose a metric for the neuron criticality of SNNs and design a regeneration mechanism to improve feature extraction and achieve efficient pruning for SNNs.
- We evaluate our method for unstructured pruning. Our method achieves higher performance compared to SOTA methods on VGG16 and ResNet19 for CIFAR100 with from 91.15% to 95.25% running cost reduction for over 90% sparsity.
- We perform the structured pruning for deep SNNs using our method, yielding better results than the sophisticated SOTA method. To our knowledge, this is the first work on structured pruning with high floating point operations (FLOPs) reduction (>50%) in deep SNNs.
- We explore the underlying impact of our method and find that: (1) our method selects critical structures with latent potential, which become more important after fine-tuning. (2) Our method improves the uniformity of class features between the train and test samples and reduces noise. These improve the stability and reduce the overfitting during the recovery phase.

2 Related Work

2.1 Network Pruning

Pruning refers to removing specific structures from a network to induce sparsity. Unstructured pruning [Han *et al.*, 2015] removes weight parameters to achieve a high level of connection sparsity. However, standard hardware does not fully optimize sparse matrix operations, limiting potential acceleration from unstructured pruning. Structured pruning [He *et al.*, 2017] achieves structured sparsity by removing entire kernels or channels. This approach is hardware-friendly but might not reach the highest sparsity.

Pruning Criterion

The most commonly employed pruning paradigm involves evaluating the impact of structure on network performance through a pruning criterion and removing the least significant ones. For unstructured pruning, the magnitude of each weight has emerged as the most widespread pruning criterion, which was firstly proposed in [Han *et al.*, 2015] and has seen widespread adoption in pruning for ANNs [Zhu and Gupta, 2017; Liu *et al.*, 2021] and SNNs [Kim *et al.*, 2022; Huang *et al.*, 2023]. The synaptic parameter [Bellec *et al.*, 2018], which represents the connection strength, is another pruning criterion. Chen *et al.* [2021] improved the synaptic parameter with gradient rewiring and applied it to SNN pruning. For structured pruning, the first and second-order information of the gradient is utilized to design importance scores [Molchanov *et al.*, 2016; He *et al.*, 2017]. Hu *et al.* [2016] proposed the average percentage of zeros (APoZs) of the activation layer output serving as a pruning criterion. Liu *et al.* [2017] proposed the scalar parameters representing channels' significance and used the penalty term to push them toward zero during training.

Pruning Schedule

The setting of pruning schedules affects the performance of pruned networks. Iterative pruning follows the pruning-fine-tuning pattern with settings such as the pruning ratio in one iteration, pruning interval, and number of iterations. Zhu and Gupta [2017] proposed a gradual sparse ratio schedule with a unified pruning interval for unstructured pruning and was followed by subsequent studies [Gale *et al.*, 2019; Liu *et al.*, 2021]. Molchanov *et al.* [2016, 2019]; Ding *et al.* [2021] implemented the iterative pruning on channel level. Frankle and Carbin [2018] proposed the lottery hypothesis with a fixed pruning ratio and a longer pruning interval while inheriting the surviving parameters of the initial model after each iteration. Kim *et al.* [2022] proved the lottery hypothesis in SNN pruning. One-shot pruning refers to achieving the target sparsity once. You *et al.* [2019] proposed using the Hamming distance of pruning masks in the early stages of training to determine the pruning time. Kim *et al.* [2022] implemented the above method on SNN pruning.

3 Preliminaries

3.1 Spiking Neural Network

In SNN, a neuron receives signals from model inputs or pre-synaptic neurons and modulates the membrane potential.

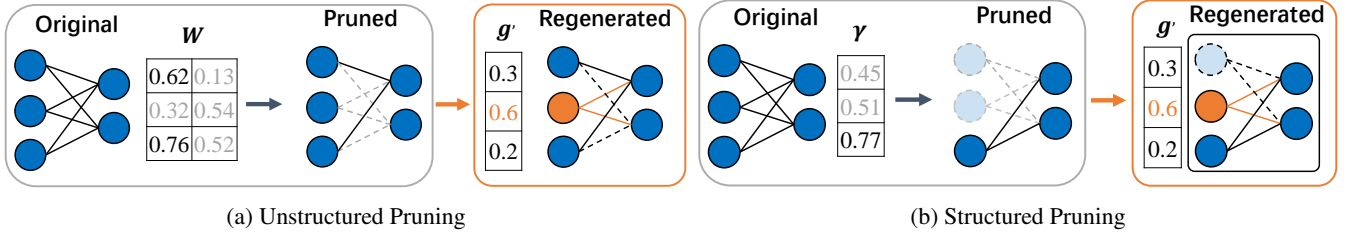


Figure 1: Schematic view of Pruning-Regeneration Process. Faded structures and connections with dotted lines are pruned. The orange ones with higher criticality scores are regenerated in our method. (a) Unstructured pruning via global magnitude pruning criterion and regeneration based on criticality. (b) Structured pruning via the scale factor γ (BN layer parameter) and regeneration based on criticality.

When the membrane potential exceeds the threshold, An output spike is generated and sent to the post-synaptic neuron. The fire process is described as:

$$s[t] = \Theta(h[t] - V_{threshold}), \quad (1a)$$

$$\Theta(x) = 0, x < 0 \text{ otherwise } 1, \quad (1b)$$

where t represents the current time step and $h[t]$ represents current membrane potential. $V_{threshold}$ is the threshold voltage. The neuron model formalizes the processes of charging and resetting of neurons. Following previous SNN works, we use the Leaky Integrate and Fire (LIF) model with a simple form and robust performance.

We employ spatio-temporal backpropagation (STBP) [Wu *et al.*, 2018] in the learning process. To address the non-differentiability issue of Eq.1b at zero, a surrogate function [Wu *et al.*, 2018, 2019; Zheng *et al.*, 2021] is commonly utilized during the backward phase to replace Eq.1b. We use

$$g(x) = \frac{1}{\pi} \arctan(\pi x) + \frac{1}{2}, \quad (2a)$$

$$g'(x) = \frac{1}{1 + \pi^2 x^2}. \quad (2b)$$

Eq.2a defines the surrogate function utilized in this study. And the derivative, Eq.2b, is employed to approximate the gradient in the backward phase.

3.2 Criticality in Neuroscience

Neuroscience suggests that the critical state plays a vital role in the brain’s efficient information processing [Beggs and Timme, 2012; Di Santo *et al.*, 2018]. This theory, known as the critical brain hypothesis [Turing, 2009], asserts that the brain operates in a critical state. In this state, the brain is highly sensitive to any input that can alter its activity. Even minimal stimuli can trigger a rapid cascade of neuronal excitation, facilitating information transmission throughout the brain and improving complex feature extraction [Kinouchi and Copelli, 2006; Beggs, 2008; Shew *et al.*, 2009; Beggs and Timme, 2012].

Previous research has observed the criticality in neural systems at different scales Hesse and Gross [2014]; Heiney *et al.* [2021]. Self-organized criticality (SOC) refers to the ability of a dynamic system to tune itself toward the critical state effectively. Herz and Hopfield [1995] first indicated a mathematical equivalence between SOC models and LIF neuron networks. Gal and Marom [2013] established the association

between SOC and the single neuron according to the experimental phenomenon. They found that the cortical neurons of newborn rats keep around a barely-excitable state, exhibiting characteristics of SOC. Activities push the neuron towards an excitatory state, while regulatory feedback pulls it back at a longer time scale.

4 Method

4.1 Criticality from Biology to SNNs

Inspired by the critical brain hypothesis, We aim to exploit the advantages of the critical state to improve SNN pruning. Specifically, we hope that pruned models retain more critical characteristics and maintain sensitivity to inputs and efficiency in feature extraction, ultimately accelerating pruning and improving post-pruning performance. We start from a single neuron to exploit the criticality in SNNs since it shows the lowest level of criticality in neuroscience [Gal and Marom, 2013]. Previous works [Hu *et al.*, 2016; Liu *et al.*, 2022] have improved pruning through properties exhibited by neurons during training and pruning processes. Drawing from these works, a natural idea is to compute the criticality score of neurons and select ones with higher criticality.

The key challenge is to find a suitable metric for neuron criticality. Gal and Marom [2013] reveal that criticality is correlated with the barely-excitable state of neurons. Plesser and Gerstner [2000]; Maass [2014] indicate that the magnitude of the membrane potential is positively correlated with the excitation probability. As the membrane potential approaches the threshold voltage, the excitation probability rapidly transitions between 0 and 1. Following this line, we propose that neuronal criticality is related to the distance between the membrane potential and the threshold voltage. The behavior of a neuron is considered to have higher criticality when the membrane potential is closer to the threshold voltage. Considering pruning and training processes, we suggest that the derivative of the surrogate function, such as g' in Eq.2b, serves as a criticality metric. It offers several advantages: (1) The derivatives of mainstream surrogate functions reach the highest value when the membrane potential equals the threshold voltage and rapidly decreases with increasing distance, effectively reflecting the criticality changes of a neuron’s behavior. (2) The derivative of the surrogate function can be directly obtained during model training with minimal additional computational cost. (3) The derivative of the surrogate function has a unified value range, enabling global ranking.

4.2 Regeneration via Neuron Criticality

We aim to develop a mechanism compatible with various pruning strategies to preserve critical neurons. To achieve this, we combine the criticality metric mentioned above with a neuron regeneration mechanism. The regeneration mechanism is inspired by synaptic regeneration in the brain and used to reactivate pruned structures. Gradient magnitude has been used as a criterion for regeneration in previous ANN pruning methods like RigL [Evci *et al.*, 2020] and GraNet [Liu *et al.*, 2021], but it lacks motivation and biological interpretability for SNNs. We implement a regeneration mechanism based on neuron criticality to maintain the critical state of the pruned model.

Specifically, to avoid the sparsity of the model after regeneration from being lower than the target, we first temporarily expand the target sparsity at the current pruning iteration s_t to s'_t :

$$s'_t = s_t + r(1 - s_t), \quad (3)$$

where t represents current pruning iteration and r is the regeneration rate. s_t is the target sparsity, and s'_t is the temp sparsity for pruning before regeneration at the current iteration. After each pruning iteration, we re-sort all pruned structures (neurons or synapses) in the pruned model based on the criticality scores of the corresponding neurons and reactivate the top k with the highest scores:

$$S_{\text{new}} = S + \text{TopK}(C(S')), \quad (4)$$

where S is the set of surviving pruning structures after the pruning iteration. S' is the set of all pruned structures. $C(x)$ denotes the criticality score of x . To compute the criticality score, we have

$$s(e) = \text{aggregate} \left(\frac{1}{T} \sum_{i=0}^T g'(u_{e,i}) \right), \quad (5a)$$

$$C(e) = \frac{1}{N} \sum_{i=1}^N s_i(e). \quad (5b)$$

Eq.5a and 5b illustrate the approach to obtaining criticality scores for a neuron e . $u_{e,i}$ represents the membrane potential of e at i th time step. T is the total number of time steps. g' is the derivative of the surrogate function. N is the total number of samples used to compute the criticality score. *aggregate* represents the way to aggregate the results for the corresponding pruning structure. For the fully connected layer, we directly compute the average criticality score for each neuron. For convolutional layers, we explore two approaches: mean aggregation and max aggregation. We finally employ max operation due to its superior performance in the experiments. We suppose that max aggregation preserves the highest response within the corresponding region, preventing robust responses from being diminished by neighboring elements within the feature map.

4.3 Overall Pruning Strategy

So far, we have known how to calculate the criticality scores of neurons. In order to evaluate the impact of preserving critical neurons on sparse SNN, we perform pruning on SNNs at

both unstructured (connection) and structured (channel) levels. As depicted in Figure 1, our approach employs the basic pruning techniques and incorporates the regeneration mechanism based on neuron criticality. We introduce the workflow below. Implementation details are contained in Appendix A.

Unstructured Pruning

To better evaluate the effectiveness of the criticality-based regeneration mechanism, we choose the simple global magnitude pruning criterion $|w|$ to achieve connection level sparsity in deep SNNs, where w is the connection weight. Following the gradual pruning scheme (details in Appendix A) in [Zhu and Gupta, 2017], we iteratively prune the network until reaching the final target sparsity and perform the regeneration based on neuron criticality after each pruning iteration. Specifically, we collect the values of $g'(u)$ from the last training iteration before pruning and calculate the average criticality score. Then, we perform the global regeneration after pruning.

Structured Pruning

We employ the scaling factor of the batch normalization layer to obtain channel-level sparse models following [Liu *et al.*, 2017] (details in Appendix A). Specifically, we leverage the parameter γ in batch normalization layers as the pruning criterion and incorporate L1 sparsity regularization during training. After training, we prune channels according to the magnitude of γ . Then, we calculate the criticality score for each channel by collecting the average values of the surrogate function derivative from the entire training dataset. Finally, we execute regeneration with criticality scores and fine-tune the pruned network.

5 Experiment

5.1 Experimental Setup

We evaluate our method on a shallow SNN(6-conv-2-fc) and two representative deep SNNs VGG-16 [Simonyan and Zisserman, 2014] and ResNet-19 [He *et al.*, 2016] for three datasets CIFAR10, CIFAR100 [Krizhevsky *et al.*, 2009] and Tiny-ImageNet [Hansen, 2015]. We use batch size 128, SGD optimizer with momentum 0.9 and learning rate 0.3. We set 200 epochs for iterative pruning for CIFAR10 and CIFAR100 (100 for tiny-ImageNet) and the timestep to 5 for all experiments. Following previous works, we use batch normalization (BN) and take the first convolutional layer as the encoder to transform the input images into spikes. Our implementation is based on PyTorch. The experiments are executed on an RTX 3090 GPU. More implementation details are contained in Appendix B.

5.2 Accuracy and Efficiency Evaluations

Unstructured Pruning

We evaluate our method in Table 2 and compare it with state-of-the-art (SOTA) pruning methods for SNNs, including Grad R [Chen *et al.*, 2021], STDS [Chen *et al.*, 2022], RigL [Evci *et al.*, 2020], IMP [Kim *et al.*, 2022], NDSNN [Huang *et al.*, 2023], and RCMO-SNN [Chen *et al.*, 2023]. We report accuracy and pruning costs at different sparsity levels. The pruning cost is estimated as $\frac{T \times N_p}{N_d}$ where T is the number of time

| Pruning Method | Dataset | Arch. | Base Acc. (%) | Cost | Pruned Acc. (%) | Sparsity (%) |
|---|---------------|------------|---------------|-------------------------|---|--|
| Grad R [Chen <i>et al.</i> , 2021] | CIFAR10 | 6Conv, 2Fc | 92.84 | 54.61 | 91.47 89.32 | 97.65 99.27 |
| STDS [Chen <i>et al.</i> , 2022] | CIFAR10 | 6Conv, 2Fc | 92.84 | - | 92.49 90.21 | 97.77 99.25 |
| RCMO-SNN [Chen <i>et al.</i> , 2023] | CIFAR10 | 6Conv, 2Fc | 92.88 | 54.61 | 92.75 90.32 | 97.71 99.31 |
| Ours | CIFAR10 | 6Conv, 2Fc | 92.79 | 3.33 | 92.77±0.21 90.45±0.16 | 97.71 99.31 |
| NDSNN [Huang <i>et al.</i> , 2023] | CIFAR100 | VGG16 | 69.86 | 5.00 | 68.07 66.73 63.51 | 90.00 95.00 98.00 |
| IMP [Kim <i>et al.</i> , 2022] | CIFAR100 | VGG16 | - | 37.67 56.33 70.33 | 68.90 68.00 66.02 | 89.91 95.69 98.13 |
| Ours | CIFAR100 | VGG16 | 72.89 | 3.33 | 72.69±0.15 72.23±0.19 70.70±0.20 | 90.00 95.69 98.13 |
| Grad R [Chen <i>et al.</i> , 2021] | CIFAR100 | ResNet19 | 71.34 | 34.13 | 67.47 67.31 | 94.92 97.65 |
| IMP [Kim <i>et al.</i> , 2022] | CIFAR100 | ResNet19 | 71.34 | 37.67 56.33 70.33 | 71.38 70.54 67.35 | 89.91 95.69 98.13 |
| RCMO-SNN [Chen <i>et al.</i> , 2023] | CIFAR100 | ResNet19 | 74.71 | 51.67 65.67 | 72.67 70.80 | 95.19 97.31 |
| Ours | CIFAR100 | ResNet19 | 74.31 | 3.33 | 73.65±0.23 73.01±0.06 71.48±0.12 | 90.00 95.19 98.13 |
| RigL [Evcı <i>et al.</i> , 2020] | Tiny-ImageNet | ResNet19 | 50.32 | 7.50 | 49.49 40.40 37.98 | 90.00 95.00 98.00 |
| NDSNN [Huang <i>et al.</i> , 2023] | Tiny-ImageNet | ResNet19 | 50.32 | 7.50 | 49.25 47.45 45.09 | 90.00 95.00 98.00 |
| IMP ¹ [Kim <i>et al.</i> , 2023] | Tiny-ImageNet | ResNet19 | 58.00 | 2.50 | 54.94 54.54 51.03 | 90.00 95.00 98.00 |
| Ours | Tiny-ImageNet | ResNet19 | 59.85 | 2.50 | 58.00±0.16 57.95±0.25 56.24±0.09 | 90.00 95.00 98.00 |

¹ We run the code from [Kim *et al.*, 2022] to obtain results of Tiny-ImageNet.

Table 2: Performance comparison between our method and previous works for unstructured pruning. The results reported with (mean±std) are run with three random seeds. We mark the best results in bold.

steps, N_p is the total number of epochs during pruning, and N_d is the number of epochs for training dense models in this work (same for all methods). The costs of different methods are normalized with N_d . On CIFAR10 with the shallow 6conv-2fc SNN, our method outperforms previous approaches at all sparsity levels with lower pruning costs. On the more complex datasets CIFAR100 and Tiny-ImageNet, our method exhibits even more significant improvements. As shown in Table 2, On CIFAR100, we achieve higher accu-

racy compared to IMP and RCMS-SNN with a pruning cost reduction ranging from 91.15% to 95.26% on VGG16 and ResNet19. For Tiny-ImageNet, our method demonstrates from 3.06% to 5.21% performance advantages over IMP with the same pruning costs.

Structured Pruning

In Table 3, we evaluate the performance of our method on CIFAR100 for structured pruning. As pioneers in implementing

| Pruning Method | Pruned Acc. (%) | FLOPs ↓ (%) |
|-----------------------------|-----------------|--------------|
| VGG16 | | |
| [Liu <i>et al.</i> , 2017] | 67.92 | 43.76 |
| | 66.24 | 58.10 |
| [Wang <i>et al.</i> , 2021] | 68.05 | 43.73 |
| | 67.13 | 58.01 |
| Ours | 68.90 | 43.76 |
| | 67.64 | 58.02 |
| ResNet19 | | |
| [Liu <i>et al.</i> , 2017] | 71.08 | 49.44 |
| | 68.34 | 69.49 |
| [Wang <i>et al.</i> , 2021] | 70.37 | 49.40 |
| | 69.20 | 69.42 |
| Ours | 71.28 | 49.46 |
| | 70.01 | 69.47 |

Table 3: Performance comparison between our method to [Liu *et al.*, 2017] and [Wang *et al.*, 2021]. We report the test accuracy of VGG16 and ResNet19 models after structured pruning on CIFAR100 and mark the best results in bold.

| Method | Sparsity | | |
|----------------------|----------|--------|--------|
| | 90.00% | 95.69% | 98.13% |
| baseline | 70.84 | 70.56 | 69.98 |
| w/neuron criticality | 72.69 | 72.23 | 70.70 |

Table 4: Test accuracy of VGG16 model with different sparsity on CIFAR100 after unstructured pruning using the baseline and proposed method.

structured pruning on SNNs, we compare our method with the SOTA works of ANN pruning NSlim [Liu *et al.*, 2017] and GReg [Wang *et al.*, 2021] and report the pruned test accuracy and the float point operations reduction (FLOPs ↓) in inference. Additionally, we take NSlim as our baseline because our method develops based on it. Our method consistently outperforms GReg [Wang *et al.*, 2021], which is more complex and computationally expensive, and shows significant improvements compared to the baseline, all while maintaining the equivalent level of FLOPs.

5.3 Effect of Neuron Criticality

We compare the baseline and pruning based on neuron criticality on CIFAR100. The results of the ablation study are shown in Table 4, where the proposed method outperforms the baseline at all sparsity levels. Furthermore, to evaluate the contribution of the criticality-based regeneration mechanism, we perform a performance analysis in Figure 2 using various regeneration metrics, including criticality, Grad Evci *et al.* [2020], Random, and GraNet [Liu *et al.*, 2021]. "Criticality" refers to the method based on criticality, "Grad" employs parameter gradients at the current iteration, "Random" adopts random ranking, and "GraNet" represents the GraNet gradient regeneration strategy. We observe that criticality-based

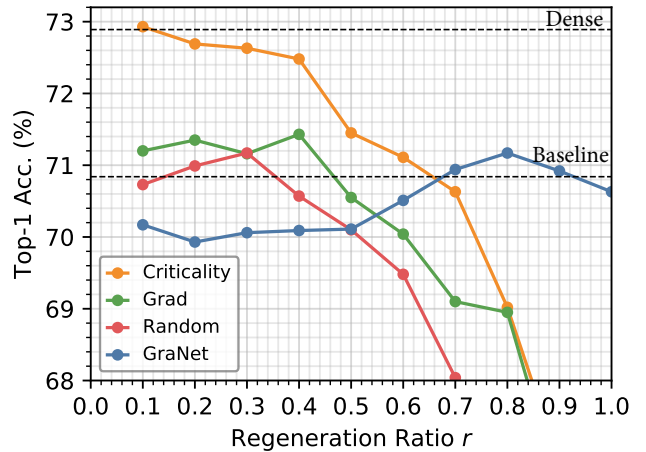


Figure 2: Comparison of regeneration methods based on criticality (ours), gradient, random, and GraNet Liu *et al.* [2021]. The two dashed lines represent the performance of the dense model and the baseline, respectively.

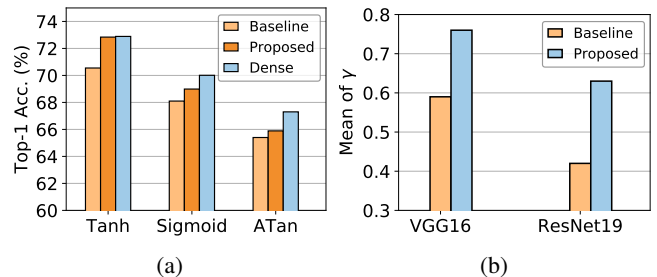


Figure 3: (a) Performance of dense model, the baseline, and the proposed method under different surrogate functions on VGG16 for CIFAR100. (b) Mean importance of non-overlapping channels between our method and the baseline for structured pruning after fine-tuning.

regeneration consistently outperforms Grad and Random regeneration, highlighting our method's superiority.

5.4 Effect of Regeneration Ratio r

To evaluate the robustness of the criticality-based regeneration, we conduct performance analysis in Figure 2 using different metrics with different regeneration ratios r . The two dashed lines represent the dense model and baseline performance, respectively. We observe that the criticality-based method exhibits stable performance within the ratio range from 0.1 to 0.6 and higher accuracy than the baseline and other methods, indicative of the robustness over the wide range of r . GraNet exhibits different performance dynamics compared to other methods. We attribute this to the cosine decay of the regeneration ratio, gradually decreasing the impact of GMP as training progresses.

5.5 Effect of Surrogate Function

To evaluate the effectiveness and robustness of the criticality mechanism for different surrogate functions, we report the pruning performance of different surrogate functions on

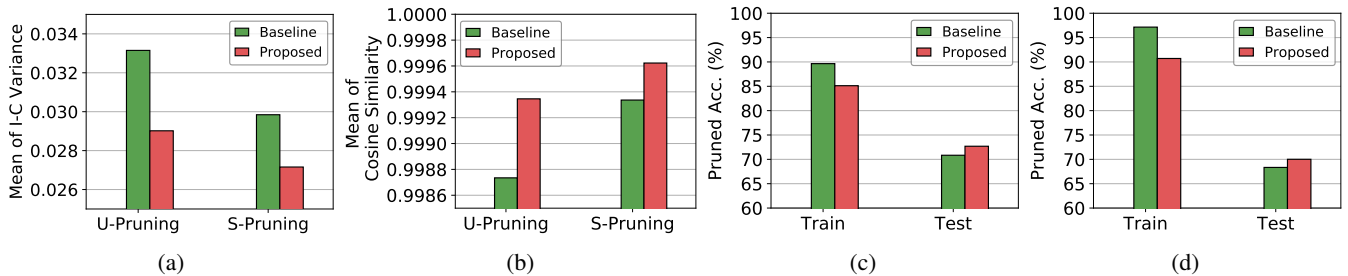


Figure 4: Comparison of the difference in feature extraction of models pruned by our method and the baseline. Our method achieves more uniform feature representations. (a) Comparison of mean of intra-cluster variance between proposed method and the baseline for VGG16 after unstructured pruning (U-Pruning) and ResNet19 after structured pruning (S-Pruning). (b) Average cosine similarity between the class feature map between the training and test dataset for VGG16 after unstructured pruning (U-Pruning) and ResNet19 after structured pruning (S-Pruning). We compare the results between the proposed method and the baseline. (c) Train accuracy and test accuracy on VGG16 for CIFAR100 after unstructured pruning using the proposed method and the baseline. (d) Train accuracy and test accuracy on ResNet19 for CIFAR100 after structured pruning using the proposed method and the baseline.

VGG16 for CIFAR100. As shown in Figure 3a, we compare three surrogate functions, tanh, sigmoid, and arc tangent, for the dense model, baseline, and proposed method. The proposed method achieves higher performance compared to the baseline across different surrogate functions. The formulas of surrogate functions are contained in Appendix B.

6 Discussion

In order to investigate the underlying impact of neuron criticality during pruning and fine-tuning, we present the experimental results and statistical findings for the pruned model in this section for more in-depth analysis.

6.1 Importance Transition

We compare the importance transition in non-overlapping surviving structures between the models obtained by our method and the baseline. To better distinguish non-overlapping structures, we focus on the results of structured pruning. In Figure 3b, we present the means of γ (normalized) of non-overlapping channels in the models through the fine-tuning process with L1 sparsity regularization for two methods. The results show that the channels regenerated by our method exhibit significantly higher importance than those without regeneration. Considering that the regenerated channels initially corresponded to lower γ values and higher criticality, this result suggests the following role of our method: identifying structures with latent potential, enabling the high-criticality structures to occupy key positions and efficiently leading to higher performance gains.

6.2 Feature Extraction

The critical brain theory suggests that the critical state of the brain promotes feature extraction and transmission. We compare the difference in feature of models pruned by our method and the baseline. Figure 4a shows the mean of intra-cluster variance [Kiang, 2001] of the features in CIFAR100 for unstructured and structured pruning, respectively. The intra-cluster variance measures the compactness of intra-cluster sample representations [Oti *et al.*, 2020]. We extract feature maps before the fully connected classifier and normalize them

to eliminate the influence of absolute values. According to Figure 4a, our model learns more consistent feature representations in almost all classes (we further report it in Appendix C) and achieves a lower mean of variances, indicating enhanced compactness in class features. This improvement is consistent for both unstructured and structured pruning.

Furthermore, Figure 4b illustrates the mean of cosine similarity of the class feature map between the training and test datasets. Our model exhibits higher similarity in feature extraction across almost all classes (we further report it in Appendix C), leading to a more uniform representation of features between the train and test samples and reducing noise. Figure 4c and 4d show the accuracies of pruned models for the training and test set after unstructured and structured pruning. Our model exhibits higher test accuracy after pruning but lower train accuracy than the baseline. We also report the training and test loss of pruned models by our method and the baseline in Appendix C, and the results demonstrate a similar pattern to Figure 4c and 4d. Combining the above observation, the baseline models suffer from overfitting during fine-tuning, and our method reduces this because the critical model learns consistent feature representation and reduces noise between training and test samples.

7 Conclusion

In this paper, inspired by the critical brain hypothesis in neuroscience, we propose a novel neuron criticality metric and design a regeneration based on criticality for high-efficiency SNN pruning. Experimental results demonstrate that our method outperforms previous SNN pruning methods in both performance and efficiency for unstructured and structured pruning. Moreover, further experiments confirm our insight that the high criticality of the pruned model improves feature extraction. An interesting future direction is to further investigate the criticality in different scales of SNNs and exploit it to guide model design and high-efficiency learning.

References

- Filipp Akopyan, Jun Sawada, Andrew Cassidy, Rodrigo Alvarez-Icaza, John Arthur, Paul Merolla, Nabil Imam, Yutaka Nakamura, Pallab Datta, Gi-Joon Nam, et al. Truenorth: Design and tool flow of a 65 mw 1 million neuron programmable neurosynaptic chip. *IEEE transactions on computer-aided design of integrated circuits and systems*, 34(10):1537–1557, 2015.
- John M Beggs and Nicholas Timme. Being critical of criticality in the brain. *Frontiers in physiology*, 3:163, 2012.
- John M Beggs. The criticality hypothesis: how local cortical networks might optimize information processing. *Philosophical Transactions of the Royal Society A: Mathematical, Physical and Engineering Sciences*, 366(1864):329–343, 2008.
- Guillaume Bellec, Darjan Salaj, Anand Subramoney, Robert Legenstein, and Wolfgang Maass. Long short-term memory and learning-to-learn in networks of spiking neurons. *Advances in neural information processing systems*, 31, 2018.
- Yanqi Chen, Zhaofei Yu, Wei Fang, Tiejun Huang, and Yonghong Tian. Pruning of deep spiking neural networks through gradient rewiring. In Zhi-Hua Zhou, editor, *Proceedings of the Thirtieth International Joint Conference on Artificial Intelligence, IJCAI-21*, pages 1713–1721. International Joint Conferences on Artificial Intelligence Organization, 8 2021. Main Track.
- Yanqi Chen, Zhaofei Yu, Wei Fang, Zhengyu Ma, Tiejun Huang, and Yonghong Tian. State transition of dendritic spines improves learning of sparse spiking neural networks. In *International Conference on Machine Learning*, pages 3701–3715. PMLR, 2022.
- Jue Chen, Huan Yuan, Jianchao Tan, Bin Chen, Chengru Song, and Di Zhang. Resource constrained model compression via minimax optimization for spiking neural networks. In *Proceedings of the 31st ACM International Conference on Multimedia*, pages 5204–5213, 2023.
- Mike Davies, Narayan Srinivasa, Tsung-Han Lin, Gautham Chinya, Yongqiang Cao, Sri Harsha Choday, Georgios Dimou, Prasad Joshi, Nabil Imam, Shweta Jain, et al. Loihi: A neuromorphic manycore processor with on-chip learning. *Ieee Micro*, 38(1):82–99, 2018.
- Lei Deng, Yujie Wu, Yifan Hu, Ling Liang, Guoqi Li, Xing Hu, Yufei Ding, Peng Li, and Yuan Xie. Comprehensive snn compression using admm optimization and activity regularization. *IEEE transactions on neural networks and learning systems*, 2021.
- Serena Di Santo, Pablo Villegas, Raffaella Burioni, and Miguel A Muñoz. Landau–ginzburg theory of cortex dynamics: Scale-free avalanches emerge at the edge of synchronization. *Proceedings of the National Academy of Sciences*, 115(7):E1356–E1365, 2018.
- Xiaohan Ding, Tianxiang Hao, Jianchao Tan, Ji Liu, Jungong Han, Yuchen Guo, and Guiguang Ding. Resrep: Lossless cnn pruning via decoupling remembering and forgetting. In *Proceedings of the IEEE/CVF International Conference on Computer Vision*, pages 4510–4520, 2021.
- Utku Evci, Trevor Gale, Jacob Menick, Pablo Samuel Castro, and Erich Elsen. Rigging the lottery: Making all tickets winners. In *International Conference on Machine Learning*, pages 2943–2952. PMLR, 2020.
- Jonathan Frankle and Michael Carbin. The lottery ticket hypothesis: Finding sparse, trainable neural networks. *arXiv preprint arXiv:1803.03635*, 2018.
- Asaf Gal and Shimon Marom. Self-organized criticality in single-neuron excitability. *Physical Review E*, 88(6):062717, 2013.
- Trevor Gale, Erich Elsen, and Sara Hooker. The state of sparsity in deep neural networks. *arXiv preprint arXiv:1902.09574*, 2019.
- Song Han, Jeff Pool, John Tran, and William Dally. Learning both weights and connections for efficient neural network. *Advances in neural information processing systems*, 28, 2015.
- Lucas Hansen. Tiny imagenet challenge submission. *CS 231N*, 5, 2015.
- Kaiming He, Xiangyu Zhang, Shaoqing Ren, and Jian Sun. Deep residual learning for image recognition. In *Proceedings of the IEEE conference on computer vision and pattern recognition*, pages 770–778, 2016.
- Yihui He, Xiangyu Zhang, and Jian Sun. Channel pruning for accelerating very deep neural networks. In *Proceedings of the IEEE international conference on computer vision*, pages 1389–1397, 2017.
- Kristine Heiney, Ola Huse Ramstad, Vegard Fiskum, Nicholas Christiansen, Axel Sandvig, Stefano Nichele, and Ioanna Sandvig. Criticality, connectivity, and neural disorder: a multifaceted approach to neural computation. *Frontiers in computational neuroscience*, 15:611183, 2021.
- Andreas VM Herz and John J Hopfield. Earthquake cycles and neural reverberations: collective oscillations in systems with pulse-coupled threshold elements. *Physical review letters*, 75(6):1222, 1995.
- Janina Hesse and Thilo Gross. Self-organized criticality as a fundamental property of neural systems. *Frontiers in systems neuroscience*, 8:166, 2014.
- Hengyuan Hu, Rui Peng, Yu-Wing Tai, and Chi-Keung Tang. Network trimming: A data-driven neuron pruning approach towards efficient deep architectures. *arXiv preprint arXiv:1607.03250*, 2016.
- Shaoyi Huang, Haowen Fang, Kaleel Mahmood, Bowen Lei, Nuo Xu, Bin Lei, Yue Sun, Dongkuan Xu, Wujie Wen, and Caiwen Ding. Neurogenesis dynamics-inspired spiking neural network training acceleration. In *2023 60th ACM/IEEE Design Automation Conference (DAC)*, pages 1–6, 2023.
- David Kappel, Stefan Habenschuss, Robert Legenstein, and Wolfgang Maass. Network plasticity as bayesian inference. *PLoS computational biology*, 11(11):e1004485, 2015.

- Melody Y Kiang. Extending the kohonen self-organizing map networks for clustering analysis. *Computational Statistics & Data Analysis*, 38(2):161–180, 2001.
- Youngeun Kim, Yuhang Li, Hyoungeob Park, Yeshwanth Venkatesha, Ruokai Yin, and Priyadarshini Panda. Exploring lottery ticket hypothesis in spiking neural networks. In *Computer Vision–ECCV 2022: 17th European Conference, Tel Aviv, Israel, October 23–27, 2022, Proceedings, Part XII*, pages 102–120. Springer, 2022.
- Youngeun Kim, Yuhang Li, Hyoungeob Park, Yeshwanth Venkatesha, Anna Hambitzer, and Priyadarshini Panda. Exploring temporal information dynamics in spiking neural networks. In *Proceedings of the AAAI Conference on Artificial Intelligence*, volume 37, pages 8308–8316, 2023.
- Osame Kinouchi and Mauro Copelli. Optimal dynamical range of excitable networks at criticality. *Nature physics*, 2(5):348–351, 2006.
- Alex Krizhevsky, Geoffrey Hinton, et al. Learning multiple layers of features from tiny images. 2009.
- Souvik Kundu, Gourav Datta, Massoud Pedram, and Peter A Beerel. Spike-thrift: Towards energy-efficient deep spiking neural networks by limiting spiking activity via attention-guided compression. In *Proceedings of the IEEE/CVF Winter Conference on Applications of Computer Vision*, pages 3953–3962, 2021.
- Zhuang Liu, Jianguo Li, Zhiqiang Shen, Gao Huang, Shoumeng Yan, and Changshui Zhang. Learning efficient convolutional networks through network slimming. In *Proceedings of the IEEE International Conference on Computer Vision (ICCV)*, Oct 2017.
- Shiwei Liu, Tianlong Chen, Xiaohan Chen, Zahra Atashgahi, Lu Yin, Huanyu Kou, Li Shen, Mykola Pechenizkiy, Zhangyang Wang, and Decebal Constantin Mocanu. Sparse training via boosting pruning plasticity with neuroregeneration. *Advances in Neural Information Processing Systems*, 34:9908–9922, 2021.
- Fangxin Liu, Wenbo Zhao, Yongbiao Chen, Zongwu Wang, and Fei Dai. Dynsnn: A dynamic approach to reduce redundancy in spiking neural networks. In *ICASSP 2022–2022 IEEE International Conference on Acoustics, Speech and Signal Processing (ICASSP)*, pages 2130–2134. IEEE, 2022.
- Wolfgang Maass. Networks of spiking neurons: the third generation of neural network models. *Neural networks*, 10(9):1659–1671, 1997.
- Wolfgang Maass. Noise as a resource for computation and learning in networks of spiking neurons. *Proceedings of the IEEE*, 102(5):860–880, 2014.
- Pavlo Molchanov, Stephen Tyree, Tero Karras, Timo Aila, and Jan Kautz. Pruning convolutional neural networks for resource efficient inference. *arXiv preprint arXiv:1611.06440*, 2016.
- Pavlo Molchanov, Arun Mallya, Stephen Tyree, Iuri Frosio, and Jan Kautz. Importance estimation for neural network pruning. In *Proceedings of the IEEE/CVF conference on computer vision and pattern recognition*, pages 11264–11272, 2019.
- Eric U Oti, SI Unyeagu, Chike H Nwankwo, Waribi K Alvan, and George A Osuji. New k-means clustering methods that minimize the total intra-cluster variance. *Afr. J. Math. Stat. Stud*, 3:42–54, 2020.
- Jing Pei, Lei Deng, Sen Song, Mingguo Zhao, Youhui Zhang, Shuang Wu, Guanrui Wang, Zhe Zou, Zhenzhi Wu, Wei He, et al. Towards artificial general intelligence with hybrid tianjic chip architecture. *Nature*, 572(7767):106–111, 2019.
- Hans E Plesser and Wulfram Gerstner. Noise in integrate-and-fire neurons: from stochastic input to escape rates. *Neural computation*, 12(2):367–384, 2000.
- Yu Qi, Jiangrong Shen, Yueming Wang, Huajin Tang, Hang Yu, Zhaohui Wu, Gang Pan, et al. Jointly learning network connections and link weights in spiking neural networks. In *IJCAI*, pages 1597–1603, 2018.
- Woodrow L Shew, Hongdian Yang, Thomas Petermann, Rajarshi Roy, and Dietmar Plenz. Neuronal avalanches imply maximum dynamic range in cortical networks at criticality. *Journal of neuroscience*, 29(49):15595–15600, 2009.
- Amar Shrestha, Haowen Fang, Daniel Patrick Rider, Zaidao Mei, and Qinru Qiu. In-hardware learning of multilayer spiking neural networks on a neuromorphic processor. In *2021 58th ACM/IEEE Design Automation Conference (DAC)*, pages 367–372. IEEE, 2021.
- Karen Simonyan and Andrew Zisserman. Very deep convolutional networks for large-scale image recognition. *arXiv preprint arXiv:1409.1556*, 2014.
- Alan M Turing. *Computing machinery and intelligence*. Springer, 2009.
- Huan Wang, Can Qin, Yulun Zhang, and Yun Fu. Neural pruning via growing regularization. In *International Conference on Learning Representations (ICLR)*, 2021.
- Yujie Wu, Lei Deng, Guoqi Li, Jun Zhu, and Luping Shi. Spatio-temporal backpropagation for training high-performance spiking neural networks. *Frontiers in neuroscience*, 12:331, 2018.
- Yujie Wu, Lei Deng, Guoqi Li, Jun Zhu, Yuan Xie, and Luping Shi. Direct training for spiking neural networks: Faster, larger, better. In *Proceedings of the AAAI conference on artificial intelligence*, volume 33, pages 1311–1318, 2019.
- Haoran You, Chaojian Li, Pengfei Xu, Yonggan Fu, Yue Wang, Xiaohan Chen, Richard G Baraniuk, Zhangyang Wang, and Yingyan Lin. Drawing early-bird tickets: Towards more efficient training of deep networks. *arXiv preprint arXiv:1909.11957*, 2019.
- Hanle Zheng, Yujie Wu, Lei Deng, Yifan Hu, and Guoqi Li. Going deeper with directly-trained larger spiking neural networks. In *Proceedings of the AAAI conference on artificial intelligence*, volume 35, pages 11062–11070, 2021.
- Michael Zhu and Suyog Gupta. To prune, or not to prune: exploring the efficacy of pruning for model compression. *arXiv preprint arXiv:1710.01878*, 2017.